The Value of Forests: Impacts on Extreme Heat and Electricity Demand *

Stefano Ramelli[†], Claudio Rizzi[‡], Simon Xu[§]

May 6, 2026

Early draft, please do not share—Comments welcome!

Abstract

Global deforestation threatens climate stability, biodiversity, and economic activity, yet the economic value of forests remains poorly understood. We provide causal evidence that forests generate significant economic benefits by offering natural protection against extreme heat. Exploiting exogenous variation in prevailing wind patterns and spatial heterogeneity in U.S. forest cover from 1985 to 2023, we show that forests reduce both local and downwind temperatures. We then document that these cooling effects translate into economically meaningful reductions in electricity demand, particularly during summer months. Finally, we discuss the implications of these findings in the context of rapidly growing energy demand from data centers. Our results highlight that forests function as a natural hedge against extreme heat, with measurable economic impacts on energy demand.

JEL Classification: Q51 Q54, Q23, G32, D22.
Keywords: Adaptation, Climate change, Electricity, Energy, Forests, Natural capital, Natural climate solutions, Temperatures.

*We thank Gernot Wagner and Emanuele Campiglio for insightful comments. This project has received funding from the European Union's 2023 research and innovation program under the Marie Skłodowska-Curie grant agreement No. 101152801. Views and opinions expressed are, however, those of the authors only and do not necessarily reflect those of the European Union or European Research Executive Agency. Neither the European Union nor the granting authority can be held responsible for them. All errors are our own.

[†]University of St.Gallen and Swiss Finance Institute, Switzerland, email: `stefano.ramelli@unisg.ch`.
[‡]IESE Business School, University of Navarra, Barcelona, Spain; email: `crizzi@iese.edu`.
[§]Harvard Business School, Harvard University, Boston, MA, United States; email: `sxu@hbs.edu`.

1 Introduction

Global deforestation has reached alarming levels, with a loss of more than 10 million hectares per year, an area the size of Portugal (e.g., FAO, 2025; WRI, 2026). This rapid decline threatens climate stability, biodiversity, and economic activity by degrading vital ecosystem services. Yet despite the scale of these risks, the welfare and economic benefits of forests remain significantly underappreciated and difficult to quantify, limiting both effective policy design and private-sector conservation and restoration efforts. Empirical identification is challenging: Forest cover is spatially non-random and evolves only gradually over time. Moreover, links between forests and other nature-related outcomes unfold over long horizons through complex ecological processes, further complicating causal inference.

In this paper, we provide novel causal evidence that forests generate material economic value by mitigating extreme heat and, in turn, reducing electricity demand. At a time of rapidly rising temperatures and electricity demand, also driven by digital technologies, the results highlight forests as a natural infrastructure that provides substantial, previously underappreciated economic benefits. Our investigation proceeds in three main steps.

First, we exploit exogenous variation in prevailing wind patterns over 1985–2023, together with geographic heterogeneity in U.S. forest cover, to identify the causal effect of upwind forests on local average monthly temperatures. We find robust evidence that forest cover substantially reduces heat exposure—both locally, through evapotranspiration and shading, and even 200 km downwind, as prevailing winds transport cooler, moisture-enriched air to nearby regions.

Second, we examine how these temperature reductions translate into electricity consumption. Consistent with the cooling effect of forests, we also find that annual increases in upwind forest cover lead to systematic declines in county-level electricity demand, especially during summer months. These findings indicate that forests act as a natural cooling system, especially when it matters most, with important implications for economic activities.

Finally, we explore the implications of our findings for the rapidly rising energy demands of data centers (IEA, 2025; Chen, 2025). Leveraging detailed geolocation data on more than 4,300 U.S. data centers as of the end of 2025, we provide evidence that forests can generate direct economic value by improving data center energy efficiency. In particular, we find that greater upwind forest exposure reduces both local temperatures and electricity demand also in areas hosting data centers.

Overall, our results show that forests provide a natural hedge against extreme heat, with economically significant effects on electricity demand. The findings carry important implications for conservation policy and for private investments in nature-based climate solutions.[1]

The paper contributes to different strands of research. First, we contribute to the literature on the climatic and environmental benefits of forests (e.g., Bonan, 2008; Bellassen

[1] According to the NGO-led initiative Reforestation Hub, as of March 2026, there are 167 million acres of low-cost reforestation opportunity in the U.S. For more information, see `https://reforestationhub.org/` and Cook-Patton et al. (2020).

and Luyssaert, 2014; Devaraju et al., 2015; Alkama and Cescatti, 2016). A large literature examines how land use and land cover influence local climate conditions, including studies on irrigation and temperature regulation (e.g., Braun and Schlenker, 2023; DeAngelis et al., 2010), crop choice and land use transformation (e.g., Loarie et al., 2011; Georgescu et al., 2011), and forestation initiatives (e.g., Alkama and Cescatti, 2016; Peng et al., 2014; Smith et al., 2023). Our focus on forests' role in mitigating heat stress builds on and extends recent work by Grosset-Touba et al. (2024), who show that the 1930s U.S. Shelterbelt afforestation program increased precipitation, reduced temperatures, and improved agricultural productivity across the Great Plains. We advance this literature by identifying a causal cooling effect of forests over the 1985–2023 period, and linking it to economically meaningful effects on electricity demand.

Second, the paper contributes to the literature on the economic consequences of degrading natural ecosystems (e.g., Costanza et al., 1997; Dasgupta, 2021; Nakhmurina et al., 2026). Despite growing attention to this issue—including in finance and economics (e.g., Flammer et al., 2025; Giglio et al., 2024; Karolyi and Tobin-de la Puente, 2023)—empirical evidence on the economic benefits of ecosystems remains limited. We contribute to this literature by providing causal evidence on the economic value of natural capital, showing that forest cover reduces electricity demand and thereby generates important, tangible economic benefits.

Finally, the paper contributes to the ongoing debate on the current and future electricity demand of data centers (e.g., IEA, 2025; Chen et al., 2025; Bogmans et al., 2026).[2] This increasing demand is also raising concerns about the potential effects of data center development on electricity prices (Benetton et al., 2023; Feher et al., 2025; Kay et al., 2026). Local climate conditions play a key role in determining data centers' cooling requirements and associated energy use (e.g., Masanet et al., 2020), as well as those of other local users, exacerbating grid stress. By showing that forests significantly reduce temperatures and electricity demand even in counties with operational, planned, or under-construction data centers, our findings highlight how natural capital can shape the energy footprint and efficiency of the digital economy in the coming decades.

2 Data

Our analyses build on high–resolution panel data covering local temperature, land cover, and atmospheric transport conditions across the conterminous United States (CONUS) from 1985 to 2023. We focus on the North American Regional Reanalysis (NARR) grid, which provides grid cells at a 32 km resolution. Table 1 reports summary statistics of the main variables used in our analyses, at the NARR grid level (Panel A) and at the county level (Panel B). In what follows, we briefly describe the main elements of our dataset.

— Table 1 —

[2] See, for instance, Forbes, "AI Is Pushing The World Toward An Energy Crisis", May 23, 2024.

Land cover

We collect the information on the spatial extent of forests and other types of land cover in the conterminous United States (CONUS) from the National Land Cover Database (NLCD).[3] This dataset includes annual remotely-sensed information on land cover across the U.S. Figure 1 shows the distributions of U.S. forest cover in 1985 and 2023, while Figure 2 illustrates the change in forest cover over the same period.

— Figures 1 and 2 —

Temperature

We collect daily temperature data from Schlenker (2024) for the period 1975–2023.[4]

We also construct the daily temperature distribution for each grid cell following the sinusoidal approximation of Snyder (1985) and using daily minimum and maximum temperatures. Specifically, for each grid cell–day, we model the daily temperature cycle as a sinusoidal function oscillating between the observed daily minimum ($T_{\min}$) and maximum ($T_{\max}$). Under this assumption, the fraction of the day during which the temperature is below a threshold T follows an arcsine distribution:

$$F(T) = \frac{1}{2} + \frac{1}{\pi} \operatorname{arcsin}! \left(\frac{T - \bar{T}}{T_{\text{amp}}} \right),$$

[3] Forest area includes evergreen, deciduous, and mixed forest classes. More details here: `https://www.mrlc.gov/data`.

[4] We match the grid cells in Schlenker (2024) (4-km resolution) to the NARR grid cells using a weighted average with the inverse of distance between the centroids of the cells from each grid system as weights.

where $\bar{T} = (T_{\min} + T_{\max})/2$ is the daily mean temperature and $T_{\text{amp}} = (T_{\max} - T_{\min})/2$ is the diurnal half-amplitude. We evaluate this CDF at the edges of 120 one-degree Celsius bins spanning $-60°$C to $+60°$C, yielding the number of hours spent in each temperature bin on each day. We aggregate daily bin-hours to monthly totals at the NARR grid level.

This procedure yields a panel of temperature percentiles at the NARR grid–year–month level, capturing not only the central tendency but also the tails of the local temperature distribution—a feature important for identifying the effects of extreme heat exposure.

Wind

Wind data are obtained from NARR eastward (u) and northward (v) 10-meter wind components.[5] For each year from 1985 to 2023, we extract daily wind fields and compute, for each NARR cell, circular mean wind direction and speed.[6] This allows us to estimate month-specific prevailing winds over the sample period.

Forest exposure measures

We construct a measure of the amount of forest area located upwind of each NARR grid cell, accounting for both the prevailing direction of atmospheric transport and the spatial pattern of land cover. Let i index NARR grid cells and let t index years. Let θ_i denote the long-run

[5] More details here:`https://psl.noaa.gov/data/gridded/data.narr.html`

[6] The circular mean is computed on the "wind-to" direction, defined as the direction toward which air flows, and the "wind-from" direction is obtained by rotating the mean direction by 180 degrees.

summer prevailing wind direction for grid i, computed as the circular mean of all available summer winds. The corresponding prevailing upwind direction is given by $\theta_i^{\text{from}} = (\theta_i + 180) \mod 360$. Around each grid cell, we draw four sector wedges: (1) an upwind wedge centered at θ_i^{from}, (2) a downwind wedge centered at θ_i, (3) two crosswind wedges centered at $\theta_i \pm 90°$. Each wedge spans $\pm 15°$ and extends to a radius of 200 km. Next, we identify the set of grid cells whose centroids lie within the upwind, downwind, and crosswind wedges, based on the wind direction.

Next, we define upwind (downwind and crosswind) forest cover by summing the hectares identified as forest across all upwind (downwind and crosswind) grid cells within 200 km.[7] Lastly, we compute local, upwind, downwind, and crosswind forest land cover changes between t and $t-1$.

Electricity consumption

We estimate electricity consumption at the county-year-month level using hourly electricity demand profiles for each CONUS county. This dataset provides estimated hourly electricity demand for each county in the CONUS from 2016 to 2023. The demand profiles represent the sum of two components: (1) weighted averages of reported hourly demand profiles for North American Electric Reliability Corporation (NERC) balancing authority (BA) regions and subregions, scaled to match annual estimates of county-level retail sales and direct use of

[7] All exposure measures are constructed for each grid–year combination.

electricity and weighted by the estimated percentage of county load served by each BA region or subregion; (2) weighted averages of modeled hourly, county- and sector-level distributed photovoltaic (DPV) capacity factor profiles, scaled to match annual estimates of on-site consumption of DPV-generated electricity for each county and weighted by the percentage of consumption attributable to each sector.

Data centers

We obtain data on U.S. data centers as of the end of 2025 from S&P Global Market Intelligence. The data cover information on around 4,300 (operational, under construction, or planned) facilities, including their type (hyperscale, retail, wholesale, and others), exact geolocations, ownership, IT space available and occupied, power capacity, and total utility power.

The distribution of data centers is relatively concentrated, with fewer than one-fifth of U.S. counties (561 out of 3,007) hosting at least one.

— Figure 4 —

Figure 4 shows the spatial distribution of operational, under construction, and planned data centers as of Q4-2025, as well as forest land cover and prevailing summer wind directions in 2023.

3 Impact on Local Temperature

Forests' cooling effects depend on their location relative to the area of interest. While local forests lower temperatures in nearby areas through evapotranspiration and shading (e.g., Bonan, 2008; Devaraju et al., 2015; Bellassen and Luyssaert, 2014; Grosset-Touba et al., 2024), winds can also transport cooler, moisture-enriched air to downwind regions, reducing temperatures well beyond the forested areas themselves.

Leveraging exogenous variations in prevailing wind direction, we compare the effects of upwind, downwind, and crosswind forest cover on local temperatures. This strategy helps isolate the cooling effect of forests while reducing concerns that the estimates are driven by endogenous local changes in forest cover or by other local shocks that affect temperatures and are correlated with forest changes. Specifically, our main empirical model is:

$$T_{ist} = \beta_1 \,\Delta\mathrm{Forest}_{ist}^{Up} + \beta_2 \,\Delta\mathrm{Forest}_{ist}^{Local} + \beta_3 \,\Delta\mathrm{Forest}_{ist}^{Down} \beta_4 + \Delta\mathrm{Forest}_{ist}^{Cross} + \gamma' X_{ist} + \mu_i + \mu_{st} + \varepsilon_{ist}, \quad (1)$$

where T_{it} is the average temperature in grid cell i in month t, in state s; $\Delta\mathrm{Forest}_{ist}^{UP}$, $\Delta\mathrm{Forest}_{ist}^{LOCAL}$, $\Delta\mathrm{Forest}_{ist}^{DOWN}$, and $\Delta\mathrm{Forest}_{ist}^{CROSS}$ represent the change in upwind, local, downwind, and crosswind forests between t and $t-1$, respectively; X_{ist} includes the change in local developed area; and μ_i and μ_{st} represent the grid cell and state-year-month fixed effects, respectively. We also construct a 500 km $\times$ 500 km grid over the CONUS and use it in place of states to control for local time-varying unobservables.

Table 2 shows the results. We find that increases in upwind forest cover lead to systematic reductions in local temperatures (columns 1 and 2). The results are robust to weighting observations using grid-cell population weights (column 3), and are significantly stronger during summer months (column 4). Importantly, yearly changes in forests located downwind have no comparable effect. This directional asymmetry is consistent with a causal channel operating through atmospheric transport rather than local confounding factors.

— Table 2 —

The cooling effect of forests appears highly non-uniform across the temperature distribution, with the strongest effects during extreme heat (column 5). The same results hold when focusing on temperatures at or above the 99th percentile, especially during summer months (column 6). Based on the estimates in column 4, a one standard deviation increase in upwind forest change (1,051 ha) results in a decrease in temperature of 0.03 degrees Celsius ((-0.256-0.058) $\times$ (1,051/10,000) = -0.03) or 0.3% of the temperature sample deviation during summer months.[8]

Figure 5 illustrates the main coefficients of interest from these regressions.

— Figure 5 —

Figure 6 reports month-by-month regression estimates. The results strongly support our interpretation: the effect of upwind forest cover is concentrated in the summer months, peaking in June.

— Figure 6 —

[8]We obtain similar results when computing changes in forest cover using a more narrow geographical focus, looking within 100 km of the grid cell's centroid, instead of 200 km. See Appendix Table IA1 and Figure IA1.

Overall, the findings in this section indicate that forests act as a natural cooling system, especially when it matters most, during periods of extreme heat. By reducing temperature spikes, forests play a crucial role in shaping local climate conditions.

4 Impact on Local Electricity Demand

Rising temperatures are a primary driver of electricity demand, particularly through increased cooling needs (e.g., Auffhammer and Mansur, 2014; Auffhammer et al., 2017). As heat exposure intensifies, electricity systems experience disproportionate demand spikes, reflecting the nonlinear relationship between temperature and cooling requirements.[9]

If upwind forest cover mitigates heat exposure, it should also reduce cooling-related electricity use, especially during the hottest periods. In Table 3, we test this prediction by regressing the natural log of county-level electricity consumption on yearly changes in forest exposure.

— Table 3 —

Consistent with the temperature results, increases in upwind forest cover lead to systematic declines in electricity demand, while forests located downwind have no comparable effect. The effect is especially pronounced during summer months (column 4), as also illustrated in Figure 8. This directional pattern supports an effect on electricity demand operating through atmospheric transport and heat mitigation.

— Figure 8 —

[9] For instance, according to EMBER (2025), U.S. electricity demand from April-September 2024 was 3.3% higher than the same period in 2023 with an estimated 37% of the increase attributed to heat waves.

Specifically, a one-standard-deviation increase in upwind forest exposure (950 hectares) reduces summer electricity demand by approximately 0.7% relative to the sample average ((-0.084 + 0.006) $\times$ (950/10,000) $\approx$ 0.007).[10] This effect is economically meaningful and reflects a substantial attenuation of heat-driven energy use. Translating this estimate into temperature-equivalent terms suggests that upwind forests offset roughly 0.2–0.5°C of effective cooling demand, based on standard reduced-form estimates of the temperature sensitivity of electricity consumption, which typically range between 1.5% and 3% per 1°C increase, with strong nonlinearities (e.g., Auffhammer et al., 2017).

At the aggregate level, these effects imply sizable economic magnitudes. Applying our estimated semi-elasticity to total U.S. electricity consumption (4.1 billion MWh in 2024), we find that a one-standard-deviation reduction in upwind forest exposure (-950 hectares within 200 km) would increase electricity demand by roughly 37 million MWh annually, corresponding to approximately $6.4 billion in additional costs at prevailing retail electricity prices ($174.50 per MWh). While this back-of-the-envelope calculation abstracts from spatial heterogeneity and equilibrium adjustments, it highlights the first-order economic importance of forests as natural cooling infrastructure.

Overall, our findings identify forests as a natural hedge not only against extreme heat but also against the resulting electricity consumption and peak demand, with direct implications for energy systems and economic activity.

[10] Land covers are scaled by 10,000.

5 Implications for Data Center Electricity Demand

Data centers are an increasingly important driver of electricity demand. Recent projections by the International Energy Agency indicate that data center electricity consumption is set to more than double by 2030, accounting for roughly one-tenth of global electricity demand growth (IEA, 2025; Chen, 2025). A substantial share of this demand is driven by cooling systems—ranging from about 7% in highly efficient hyperscale facilities to over 30% in less efficient enterprise data centers (IEA, 2025)—making local climate conditions a key determinant of data centers' energy needs (e.g., Masanet et al., 2020). At the same time, data center location decisions are shaped by a range of factors beyond climate, including local subsidies and policy incentives (Gargano and Giacoletti, 2025).

In this section, we examine whether forests can generate direct benefits by improving data center energy efficiency. On average, data centers built since 2000 are exposed to 5,830 hectares of local forest and 99,456 hectares of upwind forest within 200 km.[11] Over this period, the areas in which data centers are built experienced average annual forest losses of 26 hectares locally and 157 hectares upwind. Larger data centers, defined as those in the third quartile of installed MW capacity, are exposed to even more local and upwind forest, averaging 6,889 and 113,134 hectares, respectively. Forest loss is also greater for these data centers, with average annual losses of 28 hectares locally and 212 hectares upwind. Taken together, these patterns suggest that forest exposure is economically meaningful for data centers because of its implications for cooling demand.

Table 4 then examines whether this exposure translates into differences in local temperatures

[11]These statistics are computed using land cover in the NARR grid cell (32 km $\times$ 32 km) in which the data center is located and using summer winds.

in areas that host a data center at any point during the sample period, including locations with existing, future, or already-announced facilities. Consistent with our baseline results, increases in upwind forest cover lead to systematic reductions in local temperatures. This pattern remains robust when restricting the sample to locations with above-median data center capacity (column 3) and to extreme temperatures (column 4).

— Table 4 —

Next, Table 5 examines the effect of upwind forest exposure on electricity demand in data center counties. The results mirror our baseline findings: increases in upwind forest cover lead to systematic declines in electricity demand (columns 1 and 2), while forests located downwind have no comparable effect. Notably, this relationship appears to be concentrated in counties with higher data center capacity (column 3), suggesting that the effect is strongest in areas with the most intensive cooling demand.

— Table 5 —

Overall, these findings highlight the crucial role natural capital can play in shaping the energy footprint of the digital economy. By mitigating local heat exposure, forests can serve as decentralized climate adaptation infrastructure, with significant economic benefits for electricity demand in data-intensive sectors and, hence, for the whole economy.

6 Conclusion

In this paper, we provide evidence that forests generate significant welfare and economic value by acting as a natural hedge against extreme heat. Exploiting exogenous variation in prevailing wind patterns together with geographic heterogeneity in U.S. forest cover from 1985 to 2023, we establish a causal chain linking upwind forest exposure, local temperatures, and electricity demand.

Forests substantially reduce heat exposure in downwind areas, with effects extending more than 200 km from forest boundaries, especially in the summer months. These cooling effects translate into economically meaningful reductions in electricity demand, again, particularly during peak cooling periods. These effects also extend to counties with a significant presence of data centers, an increasingly energy-intensive sector whose electricity demand is increasingly very rapidly, potentially posing challenges for grid stability and energy prices.

The findings have several implications for policy and practice. For conservation policy, the results provide evidence that forest preservation and afforestation initiatives generate direct, measurable value for nearby areas by reducing heat exposure—a benefit distinct from carbon sequestration and biodiversity services traditionally emphasized in environmental policy and advocacy. The results also indicate that natural capital serves as an important form of decentralized climate adaptation infrastructure, significantly alleviating pressure on electricity systems and improving energy efficiency.

References

Alkama, Ramdane, and Alessandro Cescatti, 2016, Biophysical climate impacts of recent changes in global forest cover, *Science* 351, 600–604.

Auffhammer, Maximilian, Patrick Baylis, and Catherine H. Hausman, 2017, Climate change is projected to have severe impacts on the frequency and intensity of peak electricity demand across the United States, *Proceedings of the National Academy of Sciences* 114, 1886–1891.

Auffhammer, Maximilian, and Erin T. Mansur, 2014, Measuring climatic impacts on energy consumption: A review of the empirical literature, *Energy Economics* 46, 522–530.

Bellassen, Valentin, and Sebastiaan Luyssaert, 2014, Carbon sequestration: Managing forests in uncertain times, *Nature* 506, 153–155.

Benetton, Matteo, Giovanni Compiani, and Adair Morse, 2023, When technology processors come to town: High electricity use spillovers to the local economy, Working Paper.

Bogmans, Christian, Ganchimeg Ganpurev, Patricia Gomez-Gonzalez, Giovanni Melina, Andrea Pescatori, and Sneha Thube, 2026, Power hungry: How AI will drive energy demand, *Energy Economics* 109278.

Bonan, Gordon B., 2008, Forests and climate change: forcings, feedbacks, and the climate benefits of forests, *Science* 320, 1444–1449.

Braun, Thomas, and Wolfram Schlenker, 2023, Cooling externality of large-scale irrigation, Working Paper.

Chen, Sophia, 2025, Data centres will use twice as much energy by 2030—driven by AI, *Nature* .

Chen, Xin, Xiaoyang Wang, Ana Colacelli, Matt Lee, and Le Xie, 2025, Electricity demand and grid impacts of AI data centers: Challenges and prospects, Working Paper.

Cook-Patton, Susan C, Trisha Gopalakrishna, Adam Daigneault, Sara M Leavitt, Jim Platt, Sabrina M Scull, Oyut Amarjargal, Peter W Ellis, Bronson W Griscom, Jenny L McGuire, et al., 2020, Lower cost and more feasible options to restore forest cover in the contiguous united states for climate mitigation, *One Earth* 3, 739–752.

Costanza, Robert, Ralph d'Arge, Rudolf De Groot, Stephen Farber, Monica Grasso, Bruce Hannon, Karin Limburg, Shahid Naeem, Robert V. O'neill, Jose Paruelo, et al., 1997, The value of the world's ecosystem services and natural capital, *Nature* 387, 253–260.

Dasgupta, P., 2021, *The Economics of Biodiversity: The Dasgupta Review* (London: HM Treasury).

DeAngelis, Anthony, Francina Dominguez, Ying Fan, Alan Robock, M Deniz Kustu, and David Robinson, 2010, Evidence of enhanced precipitation due to irrigation over the Great Plains of the United States, *Journal of Geophysical Research: Atmospheres* 115.

Devaraju, N., Govindasamy Bala, and Angshuman Modak, 2015, Effects of large-scale deforestation on precipitation in the monsoon regions: Remote versus local effects, *Proceedings of the National Academy of Sciences* 112, 3257–3262.

EMBER, 2025, Powering through the heat: How 2024 heatwaves reshaped electricity demand, Available at `https://ember-energy.org/`.

FAO, Food and Agriculture Organization of the United Nations, 2025, Global Forest Resources Assessment, Available at `https://www.fao.org/forest-resources-assessment`.

Feher, Adam, Emilia Garcia-Appendini, and Roxana Mihet, 2025, Is AI Trained on Public Money? Evidence from US Data Centers, Working Paper.

Flammer, Caroline, Thibaud Giroux, and Geoffrey M. Heal, 2025, Biodiversity finance, *Journal of Financial Economics* 164, 103987.

Gargano, Antonio, and Marco Giacoletti, 2025, Subsidizing the cloud: U.S. state incentives to data centers, Working Paper.

Georgescu, Matei, David B. Lobell, and Christopher B. Field, 2011, Direct climate effects of perennial bioenergy crops in the United States, *Proceedings of the National Academy of Sciences* 108, 4307–4312.

Giglio, Stefano, Thorbjørn Kuchler, Johannes Stroebel, and Oliver Wang, 2024, The economics of biodiversity loss, Working Paper.

Grosset-Touba, Florian, Anna Papp, and Charles Taylor, 2024, Rain follows the forest: Land use policy, climate change, and adaptation, Working Paper.

IEA, International Energy Agency, 2025, Energy and AI, Available at `https://www.iea.org`.

Karolyi, G. Andrew, and John Tobin-de la Puente, 2023, Biodiversity finance: A call for research into financing nature, *Financial Management* 52, 231–251.

Kay, Owen, Robert Reaser, and Reid Taylor, 2026, Processing power: The effect of data centers on wholesale electricity markets, Working Paper.

Loarie, Scott R., David B. Lobell, Gregory P Asner, Qiaozhen Mu, and Christopher B. Field, 2011, Direct impacts on local climate of sugar-cane expansion in Brazil, *Nature Climate Change* 1, 105–109.

Masanet, Eric, Arman Shehabi, Nuoa Lei, Sarah Smith, and Jonathan Koomey, 2020, Recalibrating global data center energy-use estimates, *Science* 367, 984–986.

Nakhmurina, Anya, Dale T. Manning, and Eli P. Fenichel, 2026, The fiscal impact of biodiversity loss and a pathway for conservation finance, *Science* 391, 1110–1113.

Peng, Shu-Shi, Shilong Piao, Zhenzhong Zeng, Philippe Ciais, Liming Zhou, Laurent ZX Li, Ranga B Myneni, Yi Yin, and Hui Zeng, 2014, Afforestation in China cools local land surface temperature, *Proceedings of the National Academy of Sciences* 111, 2915–2919.

Schlenker, Wolfram, 2024, Daily weather data - Continental USA, available at `https://wolfram-schlenker.info/links.html`.

Smith, Callum, Eddy Robertson, Robin Chadwick, Douglas I. Kelley, Arthur P.K. Argles, Caio A.S. Coelho, Dayana C. de Souza, Paulo Y. Kubota, Isabela L. Talamoni, Dominick V. Spracklen, et al., 2023, Observed and simulated local climate responses to tropical deforestation, *Environmental Research Letters* 18, 104004.

Snyder, Richard L., 1985, Hand calculating degree days, *Agricultural and Forest Meteorology* 35, 353–358.

WRI, World Research Institute, 2026, Global Forest Review, Available at `https://www.wri.org/initiatives/global-forest-watch`.

Figures

Figure 1
Forests in the U.S.

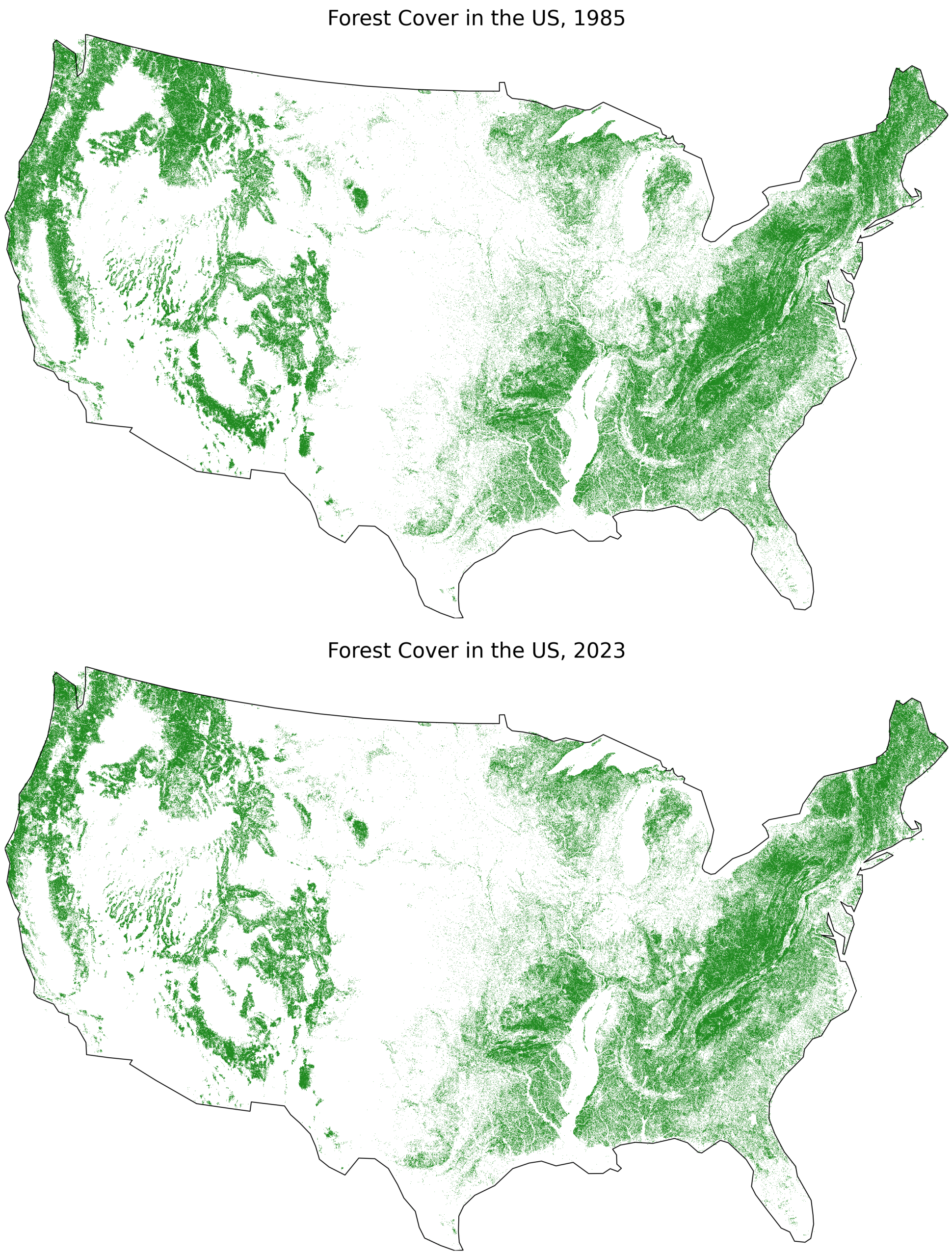

These figures report the forest cover in the CONUS for 1985 and 2023, respectively.

Figure 2
Forest cover change in the U.S.

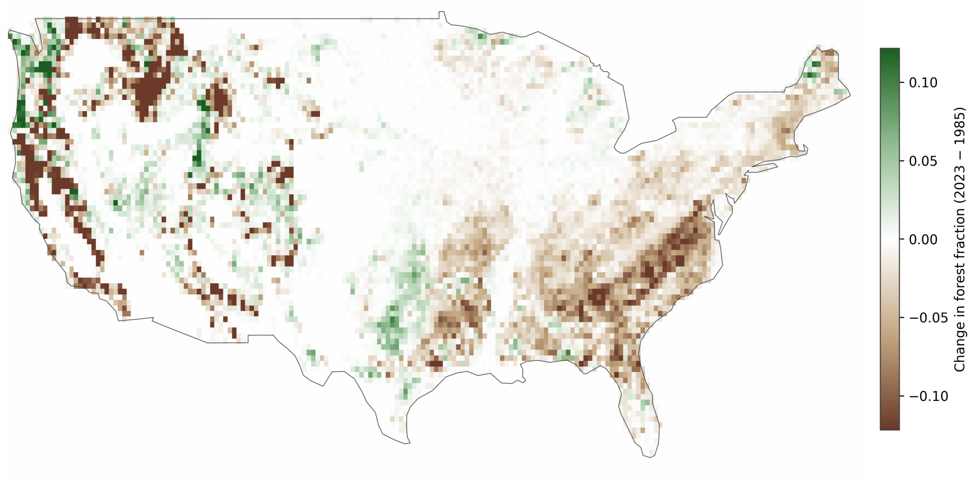

This figure reports the change in forest cover in the CONUS between 2023 and 1985.

Figure 3
Forests and wind directions.

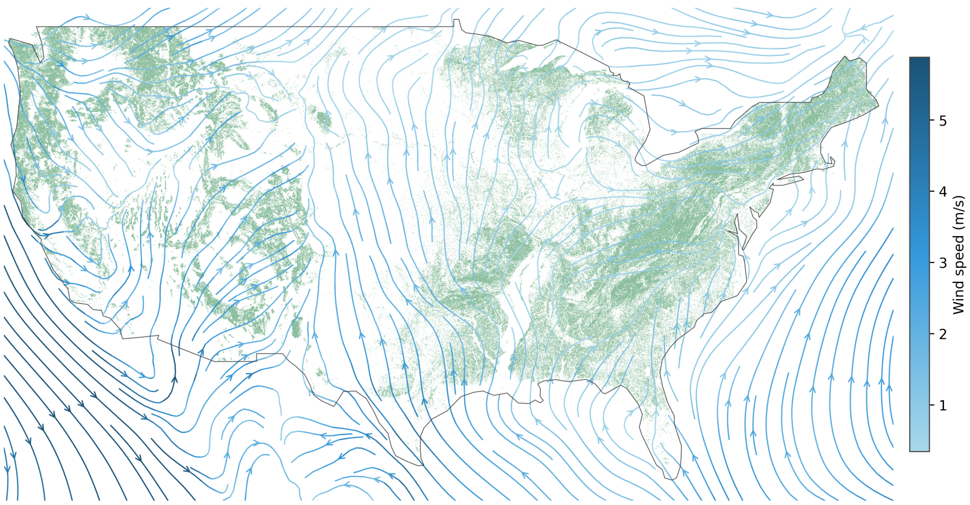

This figure reports the prevailing wind directions during summer and forest land cover in the CONUS in 2023.

Figure 4
Forests and data centers.

Panel A: Forests and operational, planned, and under construction data centers.

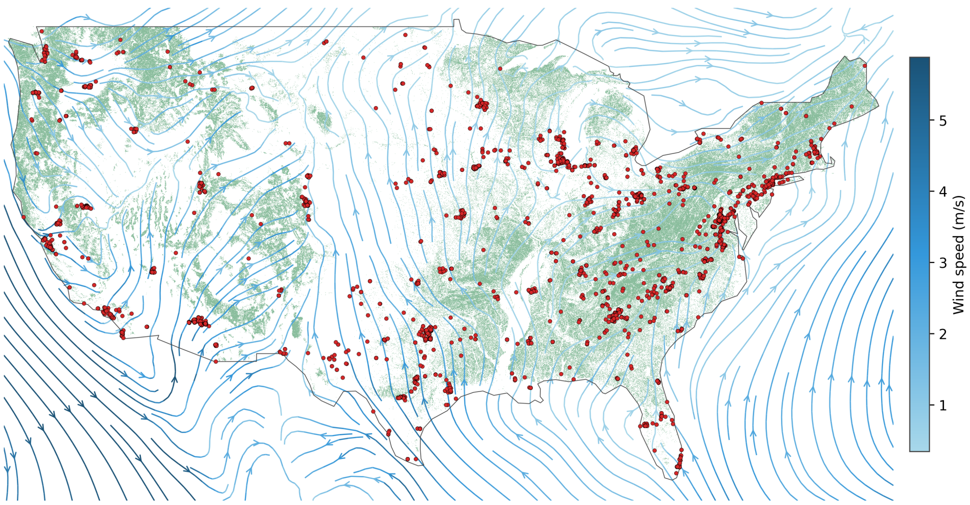

Panel B: Forests and operational data centers by size.

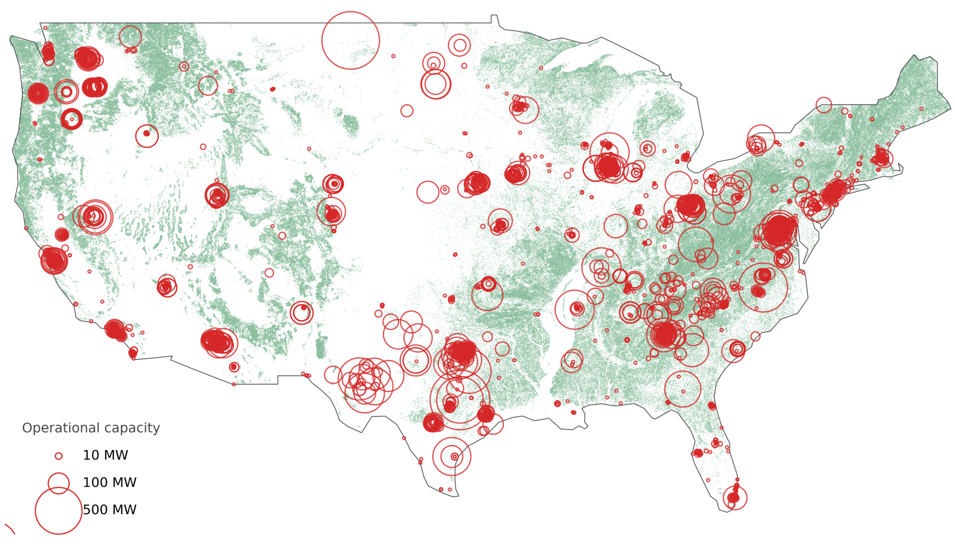

These figures show the spatial distribution of data centers, forest land cover, and prevailing summer wind directions across CONUS in 2023. In Panel A, red dots indicate the locations of operational, planned, and under-construction data centers. In Panel B, red circles indicate operational data centers, with circle size proportional to total electrical capacity in megawatts (MW).

Figure 5
Forests and temperatures.

Panel A: Upwind forests and temperatures.

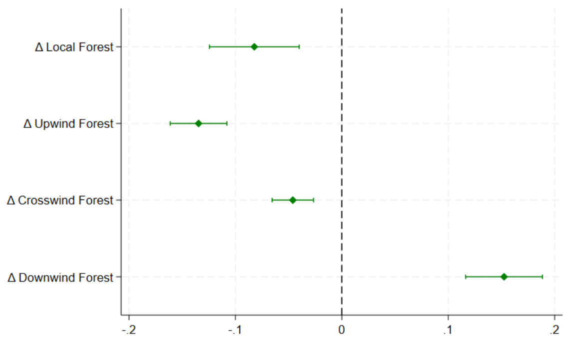

Panel B: Upwind forests and temperatures - summer months.

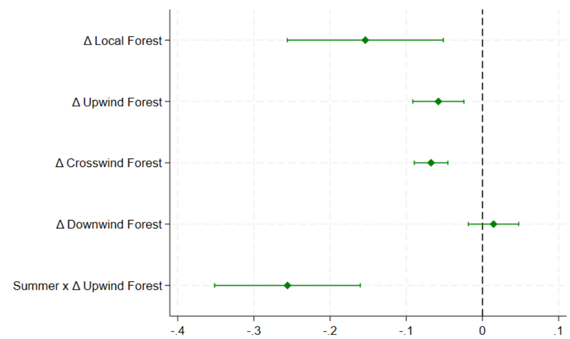

Panel C: Upwind forests and 99$^{\text{th}}$ percentile of temperatures.

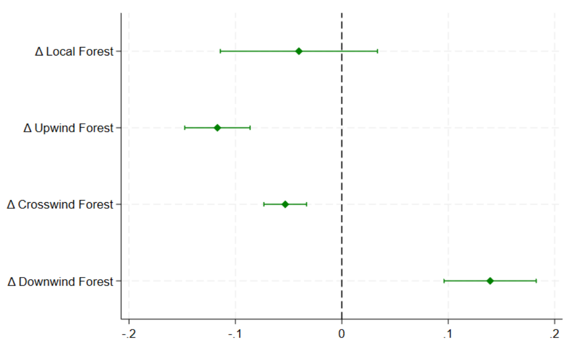

Panel D: Upwind forests and 99$^{\text{th}}$ percentile of temperatures - summer months.

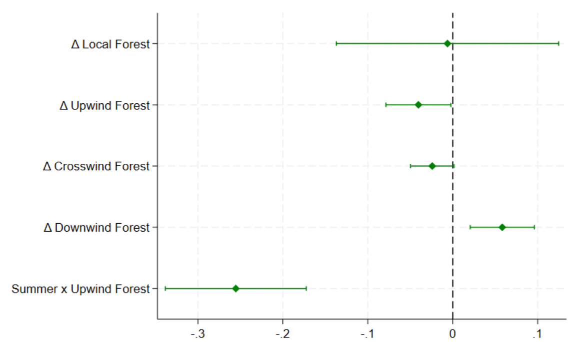

These figures report estimates from the DiD regression (eq. (1)) with average temperatures and 99th percentile temperatures as the dependent variables. All land cover changes are defined as the change between t and $t-1$ and are scaled by 10,000. Δ Local Forest denotes the change in forest area, measured in hectares, within the grid cell. Δ Upwind Forest, Δ Crosswind Forest, and Δ Downwind Forest denote the change in forest area, measured in hectares, located upwind, crosswind, and downwind of the grid cell, respectively, within 200 km of the grid cell centroid. The regressions utilize population weights. We control for changes in local developed area and include grid cell and area-year-month fixed effects. The sample excludes grid cells within 200 km of the Canada or Mexico border and spans the period 1985–2023. Standard errors are clustered at the grid cell level.

Figure 6
Forests and temperature around the year.

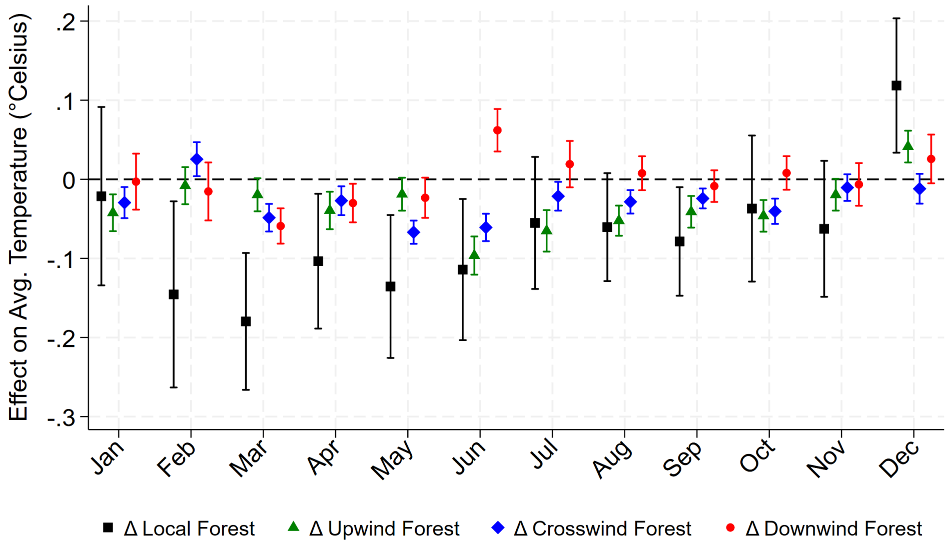

This figure reports estimates of the DiD regression (eq. (1)) with average temperatures as the dependent variable. We run separate regressions for each month. All land cover changes are defined as the change between t and $t-1$ and are scaled by 10,000. Δ Local Forest denotes the change in forest area, measured in hectares, within the grid cell. Δ Upwind Forest, Δ Crosswind Forest, and Δ Downwind Forest denote the change in forest area, measured in hectares, located upwind, crosswind, and downwind of the grid cell, respectively, within 200 km of the grid cell centroid. The regression utilizes population weights. We control for changes in local developed area and include grid cell and area-year fixed effects. The sample excludes grid cells within 200 km of the Canada or Mexico border and spans the period 1985–2023. Standard errors are clustered at the grid cell level.

Figure 7
Forests and temperature distribution.

Panel A: Upwind forests and temperature distribution.

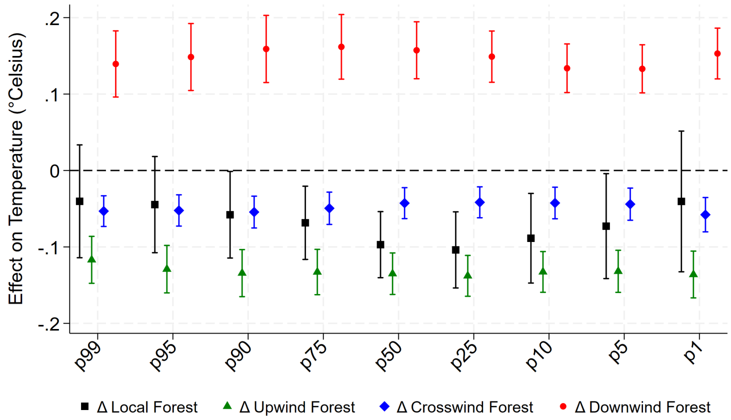

Panel B: Upwind forests and temperature distribution - summer months.

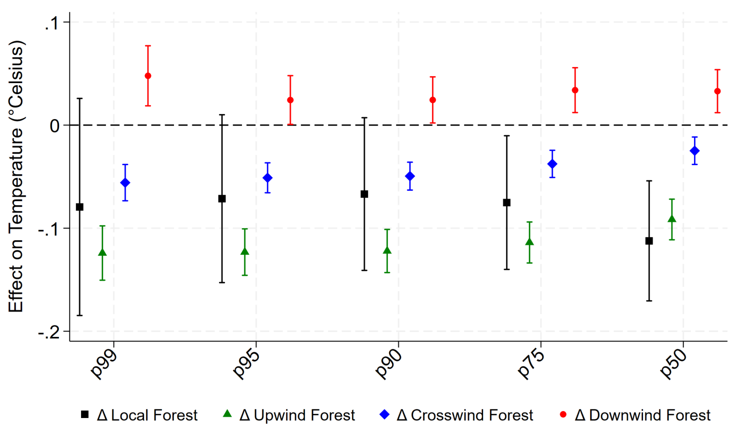

Panel A (B) reports estimates from the DiD regression in eq. (1), using different temperature percentiles as the dependent variable. Panel A uses the full sample of months, while Panel B restricts the sample to summer months. All land cover changes are defined between period $t-1$ and period t and are scaled by 10,000. Δ Local Forest denotes the change in forest area, measured in hectares, within the grid cell. Δ Upwind Forest, Δ Crosswind Forest, and Δ Downwind Forest denote the change in forest area, measured in hectares, located upwind, crosswind, and downwind of the grid cell, respectively, within 200 km of the grid cell centroid. All specifications use population weights. We control for changes in the local developed area and include grid cell and area-year-month fixed effects. The sample excludes grid cells located within 200 km of the Canadian or Mexican border. The sample period is 1985–2023. Standard errors are clustered at the cell level.

Figure 8
Upwind forests and electricity consumption.

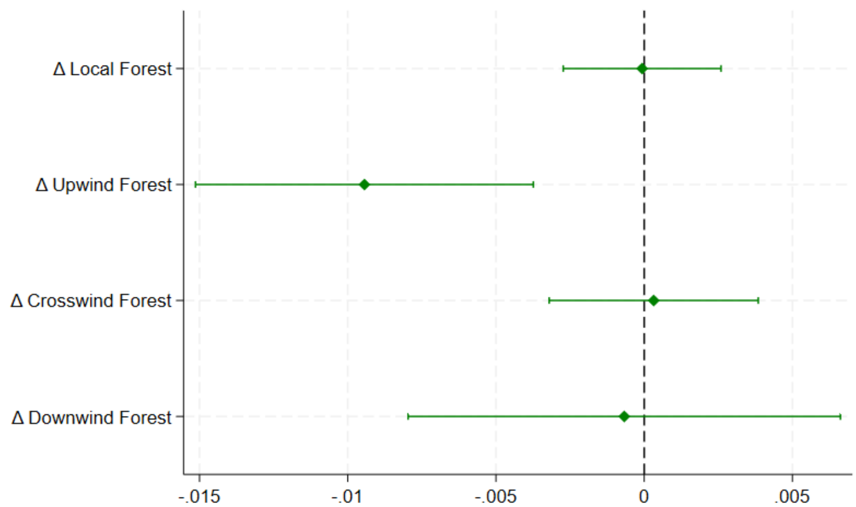

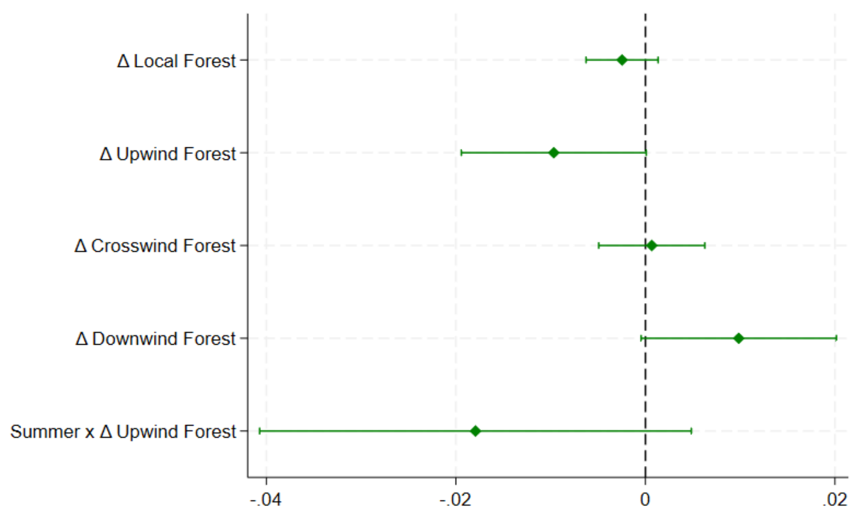

These figures report estimates of the DiD regression (eq. (1)) with electricity consumption (ln) as the dependent variable. All land cover changes are defined as the change between t and $t-1$ and are scaled by 10,000. Δ Local Forest denotes the change in forest area, measured in hectares, within the county. Δ Upwind Forest, Δ Crosswind Forest, and Δ Downwind Forest denote the change in forest area, measured in hectares, located upwind, crosswind, and downwind of the grid cell, respectively, within 200 km of the grid cell centroid. All specifications use population weights. We control for changes in local developed area, population, and personal income. We include county and state-year-month fixed effects. The sample excludes counties within 200 km of the Canada or Mexico border and spans the period 2016–2023. Standard errors are clustered at the county level.

Tables

Table 1
Summary statistics.

Panel A: Summary Statistics at the NARR grid level

	Mean	St. Dev.	Obs.	Min.	Max.
Δ Local Forest	-15	236	2,985,888	-19,873	2,890
Δ Upwind Forest w/in 200 km	-149	1,051	2,985,888	-51,935	6,679
Δ Downwind Forest w/in 200 km	-131	935	2,985,888	-60,613	6,164
Δ Crosswind Forest w/in 200 km	-303	1,535	2,985,888	-66,899	10,066
Δ Local Developed w/in 200 km	15	39	2,985,888	-394	1,416
Avg. Temp. (°C)	12	10	3,064,464	-20	37

Panel B: Summary Statistics at the NARR grid level

	Mean	St. Dev.	Obs.	Min.	Max.
Δ Local Forest	-161	2,128	255,072	-124,618	5,404
Δ Upwind Forest w/in 200 km	-158	933	255,072	-42,791	5,518
Δ Downwind Forest w/in 200 km	-152	842	255,072	-41,174	5,582
Δ Crosswind Forest w/in 200 km	-337	1,402	255,072	-40,570	8,429
Δ Local Developed	52	136	255,072	-546	3,267
Avg. Electr. Load (MW)	128	250	255,072	2	1,644
Population ('000s)	99	321	255,072	0	10,125
Personal Income ($)	46,417	14,091	223,188	18,147	406,054

This table reports summary statistics for variables used in the paper. Panels A and B report statistics at the NARR grid cell and county level, respectively. The changes in land cover are measured in hectares.

Table 2
Impact of forest changes on temperatures.

	Avg. Temp.				Temp 99th P.	
	(1)	(2)	(3)	(4)	(5)	(6)
Δ Local Forest	-0.054**	-0.080***	-0.082***	-0.154***	-0.040	-0.006
	(-2.27)	(-3.82)	(-3.83)	(-2.94)	(-1.07)	(-0.09)
Δ Upwind Forest	-0.106***	-0.130***	-0.135***	-0.058***	-0.117***	-0.040**
	(-7.62)	(-9.93)	(-9.91)	(-3.39)	(-7.46)	(-2.07)
Δ Crosswind Forest	-0.030***	-0.050***	-0.046***	-0.067***	-0.053***	-0.024*
	(-3.21)	(-5.39)	(-4.64)	(-6.00)	(-5.20)	(-1.85)
Δ Downwind Forest	0.124***	0.162***	0.152***	0.015	0.139***	0.058***
	(6.16)	(8.98)	(8.28)	(0.86)	(6.31)	(3.02)
Δ Local Developed		-0.175	-0.324	-0.308	0.184	0.197
		(-0.53)	(-0.99)	(-0.94)	(0.43)	(0.46)
Summer × Δ Upwind Forest				-0.256***		-0.255***
				(-5.25)		(-6.03)
Weights	Equal	Equal	Pop. (ln)	Pop. (ln)	Pop. (ln)	Pop. (ln)
Grid F.E.	Y	Y	Y	Y	Y	Y
State-Year-Month F.E.	Y	N	N	N	N	N
Area-Year-Month F.E.	N	Y	Y	Y	Y	Y
Observations	2,985,888	2,985,432	2,978,700	2,978,700	2,978,700	2,978,700
R^2	0.992	0.993	0.992	0.992	0.982	0.982

This table reports estimates of the DiD regressions (eq. (1)) with temperatures as the dependent variable. All land cover changes are defined as the change between t and $t-1$ and are scaled by 10,000. Δ Local Forest denotes the change in forest area, measured in hectares, within the grid cell. Δ Upwind Forest, Δ Crosswind Forest, and Δ Downwind Forest denote the change in forest area, measured in hectares, located upwind, crosswind, and downwind of the grid cell, respectively, within 200 km of the grid cell centroid. Columns (1) and (2) report the results when utilizing equal weights for each grid cell. Columns (3)-(6) report the results when utilizing population weights. We control for changes in local developed area and include grid cell and state- or area-year-month fixed effects. The sample excludes grid cells within 200 km of the Canada or Mexico border and spans the period 1985–2023. Robust t-statistics based on standard errors clustered at the grid cell level are reported in parentheses. *, **, and *** indicate significance at the 10%, 5%, and 1% level, respectively.

Table 3
Impact of forest changes on electricity consumption.

	ln(Avg. Electr. Load (MW))			
	(1)	(2)	(3)	(4)
Δ Local Forest	0.003	0.001	0.002	-0.001
	(0.63)	(0.23)	(0.41)	(-0.11)
Δ Upwind Forest	-0.019**	-0.018***	-0.016***	0.006
	(-2.17)	(-3.08)	(-2.90)	(0.66)
Δ Downwind Forest	0.000	-0.001	-0.002	0.027**
	(0.02)	(-0.22)	(-0.31)	(2.54)
Δ Crosswind Forest	-0.013**	-0.003	-0.003	0.000
	(-2.27)	(-0.92)	(-0.95)	(0.08)
Δ Local Developed	0.179**	0.178**	0.169**	0.171**
	(2.45)	(2.41)	(2.42)	(2.47)
Summer $\times$ Δ Upwind Forest				-0.084***
				(-4.79)
Weights	Equal	Equal	Pop. (ln)	Pop. (ln)
Controls	Y	Y	Y	Y
County F.E.	Y	Y	Y	Y
State-Year F.E.	Y	N	N	Y
Month F.E.	Y	N	N	Y
State-Year-Month F.E.	N	Y	Y	N
Observations	255,072	254,976	254,976	255,072
R^2	0.997	0.999	0.999	0.997

This table reports estimates of the DiD regressions (eq. (1)) with electricity consumption (ln) at the county-year-month level as the dependent variable. All land cover changes are defined as the change between t and $t-1$ and are scaled by 10,000. Δ Local Forest denotes the change in forest area, measured in hectares, within the county. Δ Upwind Forest, Δ Crosswind Forest, and Δ Downwind Forest denote the change in forest area, measured in hectares, located upwind, crosswind, and downwind of the county, respectively, within 200 km of the county centroid. Columns (1)-(2) utilize equal weights for each county. Columns (3)-(4) utilize population (ln) as weights. The control variables include changes in local developed area, population, and personal income. The sample excludes counties within 200 km of the Canada or Mexico border and spans the period 2016–2023. Robust t-statistics based on standard errors clustered at the county level are reported in parentheses. *, **, and *** indicate significance at the 10%, 5%, and 1% level, respectively.

Table 4
Impact of forest changes on temperatures in data center areas.

	Avg. Temp.			Temp 99th P.
	(1)	(2)	(3)	(4)
Δ Local Forest	-0.125	0.352	0.660	0.302
	(-0.38)	(1.06)	(1.30)	(0.46)
Δ Upwind Forest	-0.181*	-0.207**	-0.416**	-0.344*
	(-1.93)	(-2.13)	(-2.13)	(-1.82)
Δ Downwind Forest	0.210	0.156	0.067	0.095
	(1.43)	(1.36)	(0.35)	(0.50)
Δ Crosswind Forest	-0.127*	-0.158**	-0.141	-0.221*
	(-1.83)	(-2.45)	(-1.32)	(-1.97)
Δ Local Developed	-0.309	-0.878	-0.293	0.274
	(-0.36)	(-0.94)	(-0.23)	(0.15)
Sample	N. DC > 0	N. DC > 0	DC MW > p50	DC MW > p50
Grid F.E.	Y	Y	Y	Y
State-Year-Month F.E.	Y	N	N	N
Area-Year-Month F.E.	N	Y	Y	Y
Observations	243,960	243,960	109,440	109,440
R^2	0.995	0.995	0.995	0.987

This table reports estimates of the DiD regressions (eq. (1)) with temperatures as the dependent variable. All land cover changes are defined as the change between t and $t-1$ and are scaled by 10,000. Δ Local Forest denotes the change in forest area, measured in hectares, within the grid cell. Δ Upwind Forest, Δ Crosswind Forest, and Δ Downwind Forest denote the change in forest area, measured in hectares, located upwind, crosswind, and downwind of the grid cell, respectively, within 200 km of the grid cell centroid. The sample in columns (1) and (2) includes grid cells that host a data center at any point during the sample period, including locations with existing, future, or already-announced facilities. The sample in columns (3) and (4) includes grid cells with a total data center utility power above the median. This median is computed using the sample of grid cells with at least one data center. We control for changes in local developed area and include grid cell and state- or area-year-month fixed effects. The sample excludes grid cells within 200 km of the Canada or Mexico border and spans the period 1985–2023. Robust t-statistics based on standard errors clustered at the grid cell level are reported in parentheses. *, **, and *** indicate significance at the 10%, 5%, and 1% level, respectively.

Table 5

Impact of forest changes on electricity consumption in data center counties.

	ln(Avg. Electr. Load (MW))		
	(1)	(2)	(3)
Δ Local Forest	0.001	-0.007	-0.001
	(0.43)	(-1.22)	(-0.66)
Δ Upwind Forest	-0.010**	-0.013**	0.001
	(-2.55)	(-2.45)	(0.13)
Δ Downwind Forest	-0.002	-0.011	0.007
	(-0.54)	(-1.54)	(1.38)
Δ Crosswind Forest	-0.002	-0.010	-0.003
	(-0.69)	(-1.23)	(-0.88)
Δ Local Developed	0.105*	0.171**	0.110*
	(1.72)	(2.32)	(1.91)
Δ Upwind Forest $\times$ DC MW (ln)			-0.002*
			(-1.67)
Sample	N. DC > 0	DC MW > p50	N. DC > 0
Controls	Y	Y	Y
County-Month F.E.	Y	Y	Y
State-Year F.E.	Y	Y	Y
Observations	43,680	17,376	34,368
R^2	0.999	0.999	0.999

This table reports estimates of the DiD regressions (eq. (1)) with average electricity consumption at the county-year-month level as the dependent variable. All land cover changes are defined as the change between t and $t-1$ and are scaled by 10,000. Δ Local Forest denotes the change in forest area, measured in hectares, within the county. Δ Upwind Forest, Δ Crosswind Forest, and Δ Downwind Forest denote the change in forest area, measured in hectares, located upwind, crosswind, and downwind of the county, respectively, within 200 km of the county centroid. The sample in columns (1) and (3) includes counties that host a data center at any point during the sample period, including locations with existing, future, or already-announced facilities. The sample in column (2) includes counties with total data center utility power above the median. The control variables include changes in local developed area, population, and personal income. The sample excludes counties within 200 km of the Canada or Mexico border and spans the period 2016–2023. Robust t-statistics based on standard errors clustered at the county level are reported in parentheses. *, **, and *** indicate significance at the 10%, 5%, and 1% level, respectively.

Internet Appendix

Figure IA1

Forests and temperatures: robustness.

Panel A: Upwind forests and temperatures.

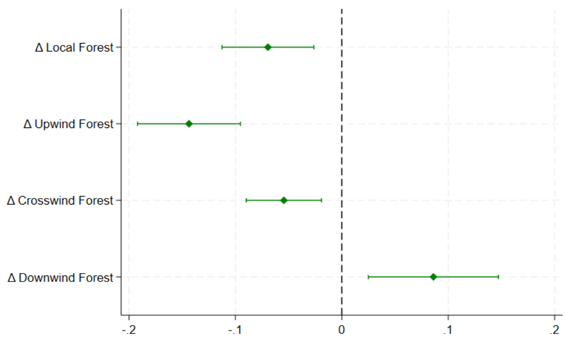

Panel B: Upwind forests and temperatures - summer months.

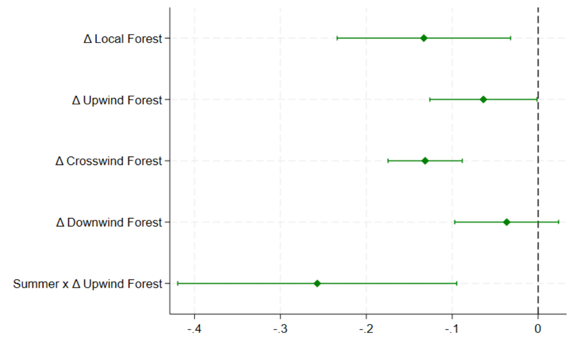

Panel C: Upwind forests and 99^{th} percentile of temperatures.

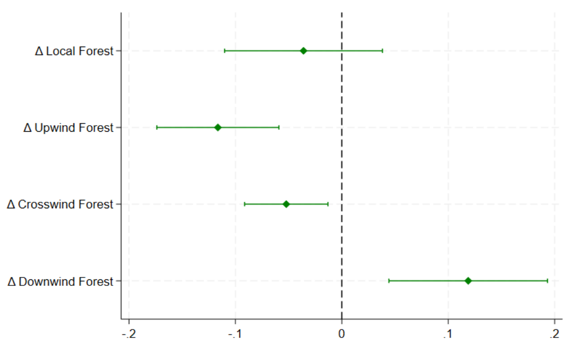

Panel D: Upwind forests and 99^{th} percentile of temperatures - summer months.

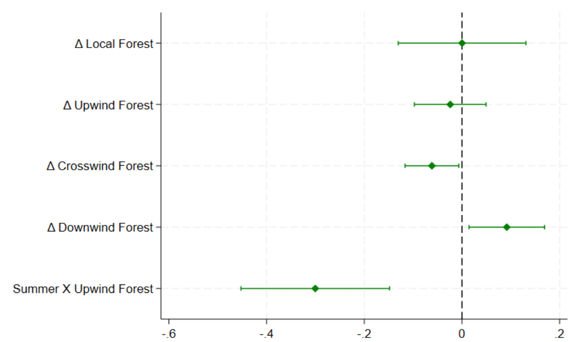

These figures report estimates from the DiD regression (eq. (1)) with average temperatures and 99^{th} percentile temperatures as the dependent variables. All land cover changes are defined as the change between t and $t-1$ and are scaled by 10,000. Δ Local Forest denotes the change in forest area, measured in hectares, within the grid cell. Δ Upwind Forest, Δ Crosswind Forest, and Δ Downwind Forest denote the change in forest area, measured in hectares, located upwind, crosswind, and downwind of the grid cell, respectively, within 100 km of the grid cell centroid. The regressions utilize population weights. We control for changes in local developed area and include grid cell and area-year-month fixed effects. The sample excludes grid cells within 200 km of the Canada or Mexico border and spans the period 1985–2023. Standard errors are clustered at the grid cell level.

Figure IA2

Forests and temperature around the year: robustness.

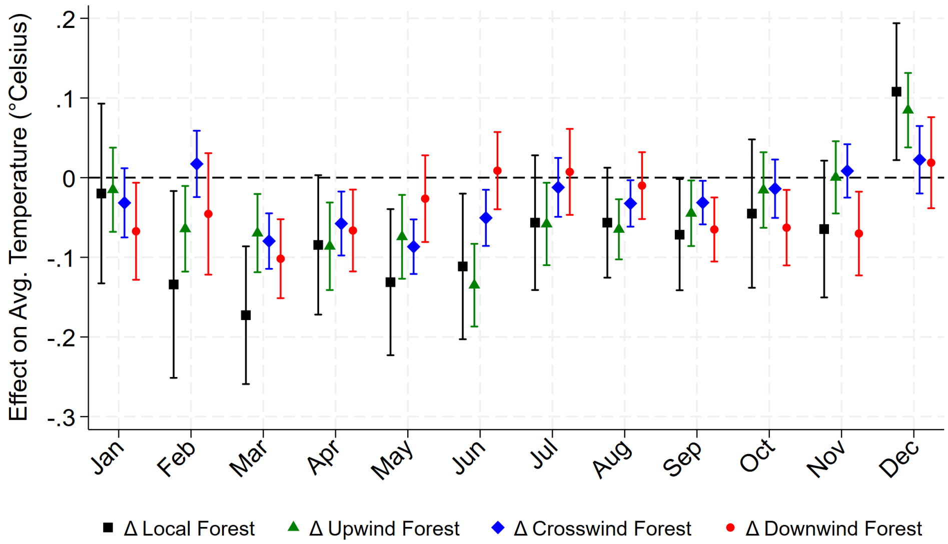

This figure reports estimates of the DiD regression (eq. (1)) with average monthly temperatures as the dependent variable. We run separate regressions for each month. All land cover changes are defined as the change between t and $t-1$ and are scaled by 10,000. Δ Local Forest denotes the change in forest area, measured in hectares, within the grid cell. Δ Upwind Forest, Δ Crosswind Forest, and Δ Downwind Forest denote the change in forest area, measured in hectares, located upwind, crosswind, and downwind of the grid cell, respectively, within 100 km of the grid cell centroid. The regression utilizes population weights. We control for changes in local developed area and include grid cell and area-year fixed effects. The sample excludes grid cells within 200 km of the Canada or Mexico border and spans the period 1985–2023. Standard errors are clustered at the county level.

Figure IA3

Forests and temperature distribution: robustness.

Panel A: Upwind forests and temperature distribution.

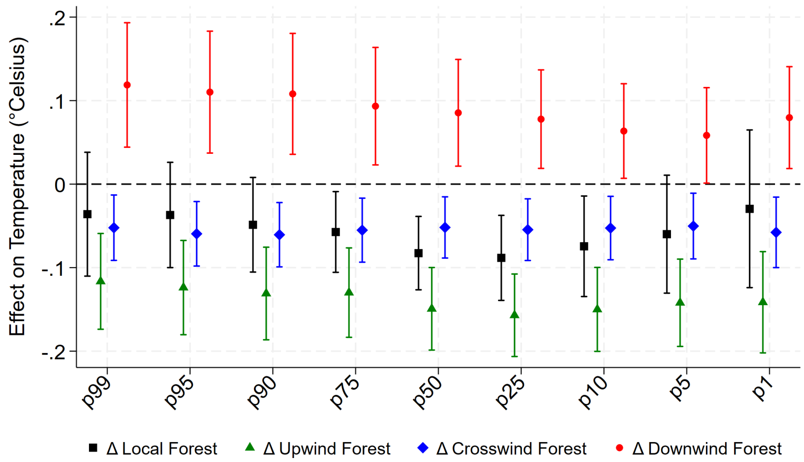

Panel B: Upwind forests and temperature distribution - summer months.

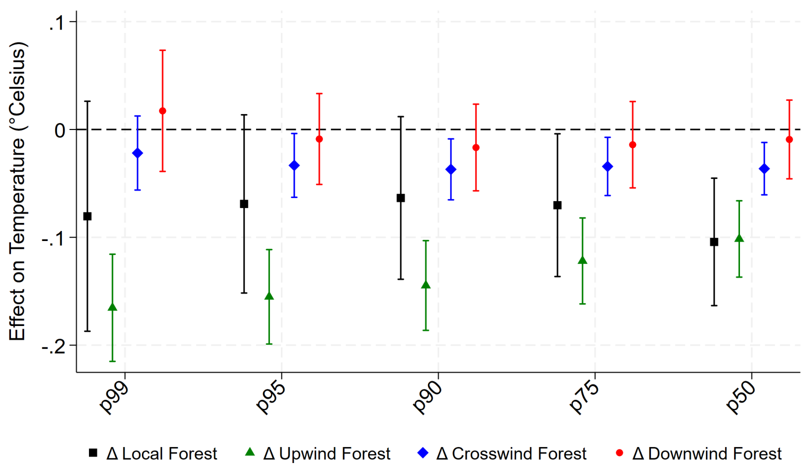

Panel A (B) reports estimates from the DiD regression in eq. (1), using different temperature percentiles as the dependent variable. Panel A uses the full sample of months, while Panel B restricts the sample to summer months. All land cover changes are defined between period $t-1$ and period t and are scaled by 10,000. Δ Local Forest denotes the change in forest area, measured in hectares, within the grid cell. Δ Upwind Forest, Δ Crosswind Forest, and Δ Downwind Forest denote the change in forest area, measured in hectares, located upwind, crosswind, and downwind of the grid cell, respectively, within 100 km of the grid cell centroid. All specifications use population weights. We control for changes in local developed area and include grid cell and area-year-month fixed effects. The sample excludes grid cells located within 200 km of the Canadian or Mexican border. The sample period is 1985–2023. Standard errors are clustered at the county level.

Table IA1
Impact of forest changes on temperatures: robustness.

	Avg. Temp.				Temp 99th P.	
	(1)	(2)	(3)	(4)	(5)	(6)
Δ Local Forest	-0.048**	-0.066***	-0.069***	-0.133***	-0.036	0.000
	(-1.99)	(-3.09)	(-3.15)	(-2.58)	(-0.95)	(0.00)
Δ Upwind Forest	-0.076***	-0.136***	-0.144***	-0.064**	-0.116***	-0.024
	(-2.93)	(-5.78)	(-5.83)	(-2.00)	(-3.98)	(-0.64)
Δ Crosswind Forest	-0.050***	-0.058***	-0.054***	-0.131***	-0.052***	-0.061**
	(-2.93)	(-3.41)	(-3.02)	(-5.97)	(-2.61)	(-2.19)
Δ Downwind Forest	0.076**	0.092***	0.086***	-0.037	0.119***	0.092**
	(2.33)	(3.16)	(2.76)	(-1.18)	(3.12)	(2.33)
Δ Local Developed		-0.192	-0.344	-0.341	0.170	0.172
		(-0.58)	(-1.05)	(-1.04)	(0.40)	(0.40)
Summer × Δ Upwind Forest				-0.257***		-0.300***
				(-3.10)		(-3.87)
Weights	Equal	Equal	Pop. (ln)	Pop. (ln)	Pop. (ln)	Pop. (ln)
Grid F.E.	Y	Y	Y	Y	Y	Y
State-Year-Month F.E.	Y	N	N	N	N	N
Area-Year-Month F.E.	N	Y	Y	Y	Y	Y
Observations	2,985,888	2,985,432	2,978,700	2,978,700	2,978,700	2,978,700
R^2	0.992	0.993	0.992	0.992	0.982	0.982

This table reports estimates of the DiD regressions (eq. (1)) with average monthly temperatures as the dependent variable. All land cover changes are defined as the change between t and $t-1$ and are scaled by 10,000. Δ Local Forest denotes the change in forest area, measured in hectares, within the grid cell. Δ Upwind Forest, Δ Crosswind Forest, and Δ Downwind Forest denote the change in forest area, measured in hectares, located upwind, crosswind, and downwind of the grid cell, respectively, within 100 km of the grid cell centroid. Columns (1) and (2) report the results when utilizing equal weights for each grid cell. Columns (3)-(6) report the results when utilizing population weights. We control for changes in local developed area and include grid cell and state- or area-year-month fixed effects. The sample excludes grid cells within 200 km of the Canada or Mexico border and spans the period 1985–2023. Robust t-statistics based on standard errors clustered at the grid cell level are reported in parentheses. *, **, and *** indicate significance at the 10%, 5%, and 1% level, respectively.